Received: 21 March 2023 | Revised: 11 July 2023 | Accepted: 4 August 2023

DOI: 10.1002/nbm.5030

RESEARCH ARTICLE

NMR IN BIOMEDICINE WILEY

Evaluation of alterations in interstitial fluid dynamics in cases of whole-brain radiation using the diffusion-weighted image analysis along the perivascular space method

Toshiaki Taoka[1,2] | Rintaro Ito[1,2] | Rei Nakamichi[2] | Toshiki Nakane[2] | Mariko Kawamura[2] | Shunichi Ishihara[2] | Kazushige Ichikawa[3] | Hisashi Kawai[4] | Shinji Naganawa[2]

[1]Department of Innovative Biomedical Visualization (iBMV), Nagoya University, Nagoya, Japan

[2]Department of Radiology, Nagoya University, Nagoya, Japan

[3]Department of Radiological Technology, Nagoya University Hospital, Nagoya, Japan

[4]Department of Radiology, Aichi Medical University, Nagakute, Japan

Correspondence
Toshiaki Taoka, Department of Innovative Biomedical Visualization (iBMV), Nagoya University Graduate School of Medicine, 65 Tsurumai-cho, Showa-ku, Nagoya, Aichi 466-8550, Japan.
Email: ttaoka@med.nagoya-u.ac.jp

Funding information
Canon Medical Systems Corporation; KAKENHI, Grant/Award Number: 21K07563

Abstract

In the current study, we assessed changes in interstitial fluid dynamics resulting after whole-brain radiotherapy using the diffusion-weighted image analysis along the perivascular space (DWI-ALPS) method, which is a simplified variation of the diffusion tensor image ALPS (DTI-ALPS) method using diffusion-weighted imaging (DWI) with orthogonal motion-probing gradients (MPGs). This retrospective study included 47 image sets from 22 patients who underwent whole-brain radiotherapy for brain tumors. The data for the normal control group comprised 105 image sets from 105 participants with no pathological changes. DWI was performed with the three MPGs applied in an orthogonal direction to the imaging plane, and apparent diffusion coefficient images for the *x*-, *y*-, and *z*-axes were retrospectively generated. The ALPS index was calculated to quantify interstitial fluid dynamics. The independent *t*-test was used to compare the ALPS index between normal controls and patients who underwent whole-brain radiotherapy. Patients were compared in all age groups and individual age groups (20–39, 40–59, and 60–84 years). We also examined the correlation between biologically equivalent doses (BEDs) and the ALPS index, as well as the correlation between white matter hyperintensity and the ALPS index. In the comparison of all age groups, the ALPS index was significantly lower ($p < 0.001$) in the postradiation group (1.32 ± 0.16) than in the control group (1.44 ± 0.17), suggesting that interstitial fluid dynamics were altered in patients following whole-brain radiotherapy. Significant age group differences were found (40–59 years: $p < 0.01$; 60–84 years: $p < 0.001$), along with a weak negative correlation between BEDs ($r = -0.19$) and significant correlations between white matter hyperintensity and the ALPS index ($r = -0.46$ for periventricular white matter, $r = -0.38$ for deep white matter). It was concluded that the ALPS method using DWI with orthogonal MPGs

Abbreviations: AC-PC, anterior commissure to posterior commissure; ADC, apparent diffusion coefficient; AQP4, aquaporin 4; BBB, blood–brain barrier; BED, biologically equivalent dose; CNS, central nervous system; DTI-ALPS, diffusion tensor image analysis along the perivascular space; DWI-ALPS, diffusion-weighted image analysis along the perivascular space; DWM, deep white matter; MPG, motion-probing gradient; PVWM, periventricular white matter.

suggest alteration in interstitial fluid dynamics in patients after whole-brain radiotherapy. Further systematic prospective studies are required to investigate their association with cognitive symptoms.

KEYWORDS
ALPS method, DWI-ALPS method, glymphatic system, interstitial fluid dynamics, MRI, neurofluids, radiotherapy, whole-brain radiation

1 | INTRODUCTION

Whole-brain radiotherapy is performed for malignant diseases such as metastatic brain tumors and primary malignant lymphomas of the central nervous system (CNS). By irradiating the entire brain, multiple tumors can be simultaneously treated. Such treatment is expected to prevent metastasis, relieve symptoms, and improve the prognosis of patients.[1,2] Recent advances in multimodal therapy have improved the survival rates in many cases of malignancy in the CNS. Consequent to improved survival, attention has been focused on long-term treatment-related morbidities. The impact of radiotherapy on the long-term cognitive performance of patients is of particular interest. The risk of cognitive symptoms following whole-brain radiation therapy has been reported to be associated with high dose, large fraction size, large radiation field, and age at treatment.[3]

Regarding interstitial fluid dynamics, the concept of the glymphatic system and neurofluids has recently been shown to be important in maintaining interstitial fluid dynamics in the brain and brain homeostasis.[4–6] The glymphatic system hypothesis is summarized as follows. The perivascular space functions as a conduit for cerebrospinal fluid to flow into the brain parenchyma. Cerebrospinal fluid directed into the perivascular space around the arteries enters the interstitial space of brain tissue through water channels controlled by aquaporin 4 (AQP4) distributed on the foot processes of astrocytes that make up the outer wall of the perivascular space. Cerebrospinal fluid entering the interstitial space flushes out waste proteins in the tissue. The driving force of this process is arterial pulsation. The cerebrospinal fluid that has flushed the intercellular spaces now flows into the perivascular space around the veins and drains out of the brain.[4] Therefore, the perivascular space plays an important role as an underlying structure related to the excretion of waste products in the brain.

The diffusion tensor image analysis along the perivascular space (DTI-ALPS) method has been introduced as an indirect, noninvasive method to evaluate interstitial fluid dynamics and has been applied in many studies.[7–18] The DTI-ALPS method yields the ALPS index, which is the ratio of the diffusivity in the direction of the perivascular space to the diffusivity in the direction perpendicular to both the major fiber tract and perivascular space, based on a special spatial relationship in the fiber tracts and the perivascular space in the axial imaging plane at the corona radiata. Although this method possesses various limitations, it is one of the methods currently available to evaluate interstitial fluid dynamics in clinical cases by providing the ALPS index as a biomarker. And the DTI-ALPS method is an effective method when used with due consideration of its limitations.[13]

The diffusion-weighted image analysis along the perivascular space (DWI-ALPS) method was introduced as a simplified version of the DTI-ALPS method.[14] The DWI-ALPS method can provide the ALPS index using diffusion-weighted images by applying motion-probing gradients (MPGs) in orthogonal directions to the imaging plane that is arranged in the anterior commissure to posterior commissure (AC-PC) line. It is known that the AC-PC plane and pyramidal tracts are orthogonal to each other.[19] When diffusion-weighted images are acquired by applying orthogonal MPG in the AC-PC plane, the direction of MPG and pyramidal tract are orthogonal on the image including the lateral ventricular body. This makes it possible to calculate the ALPS index. Diffusion-weighted imaging (DWI) is easier to perform in daily clinical practice instead of the more time-consuming diffusion tensor imaging (DTI). The ALPS index values from 12-axis DTI and three-axis DWI were reported as showing a good correlation ($r = 0.86$).[13] In this retrospective study, the DWI-ALPS method was used to evaluate changes in cerebral interstitial fluid dynamics in patients who underwent whole-brain radiation, and the relationships between age, dose, duration after radiation, and white matter hyperintensity on T2-weighted images (i.e., the Fazekas scale) were evaluated.

2 | EXPERIMENTAL METHODS

2.1 | Participants

The participants were divided into two groups. One group consisted of patients who received whole-brain radiation for malignant lesions and underwent MRI studies including DWI with orthogonal MPGs from November 2020 to December 2022 after providing written informed consent for imaging (the postradiation group). The other group comprised patients who underwent clinical MRI studies including DWI with orthogonal MPG and were found to have no abnormal findings in the brain upon MRI from November 2020 to September 2021 after providing written informed consent for imaging (the normal control group).

The data for the postradiation group (age range: 25–79 years, mean: 59.2 ± 14.9 years; male: 10, female: 12) consisted of 47 imaging sets from 22 cases after whole-brain radiation. The diseases for which whole-brain radiotherapy was applied were as follows: metastatic brain tumors from lung cancer ($n = 10$), metastatic brain tumors from breast cancer ($n = 5$), primary CNS lymphoma ($n = 4$), malignant glioma ($n = 2$), and germinoma ($n = 1$). The cases were retrospectively included from the imaging diagnosis database. Fifty-eight consecutive sets of images were initially extracted from the database, and the sets of images with the following conditions were excluded from the cohort based on clinical information: (1) imaging more than 5 years after radiotherapy ($n = 3$); and (2) imaging before the completion of radiotherapy ($n = 3$). Images of: (1) poor image quality ($n = 1$); (2) tumors or edema within the imaging plane, including the body of the lateral ventricle ($n = 2$); or (3) a large tumor causing a mid-line shift ($n = 2$), were also excluded (Figure 1).

The data for the normal control group (age range: 21–84 years, mean age: 49.9 ± 18.5 years; male: 50, female: 55) consisted of 105 imaging sets from 105 cases, which were already part of previously published data for participants aged older than 20 years.[14] The reasons for MRI were as follows: headache ($n = 15$), psychological abnormality ($n = 17$), visual abnormality ($n = 5$), screening for metastasis ($n = 26$), screening for aneurysm ($n = 38$), and follow-up for aneurysms less than 3 mm ($n = 4$). The age and sex distribution of the normal control and the postradiation groups are provided in Table 1.

2.2 | Imaging

2.2.1 | Image acquisition

Images were acquired using a 3-T clinical scanner (Vantage Centurian, Canon Medical Systems, Tochigi, Japan) equipped with a 32-channel SPEEDER coil. The DWI included in the clinical sequence was as follows: echo-planar imaging; repetition time, 5000 ms; echo time, 85 ms; SPEEDER factor, 3.0; echo train length (ETL), 64; acquisition matrix, 160 × 192; reconstruction matrix, 384 × 384; field of view (FOV), 20 cm MPG, three axes; *b*-value, 1000 s/mm^2; number of averages, one for $b = 0$ and two for $b = 1000$; acquisition time, 1 min 11 s; and axial imaging plane on the AC-PC line. The three MPGs were orthogonal to each other, with the *x*- and *y*-axes applied in the imaging plane on the AC-PC line and the *z*-axis applied orthogonal to the imaging plane on the AC-PC line. Conventional T2-weighted images were acquired using the following image sequence: fast spin echo;

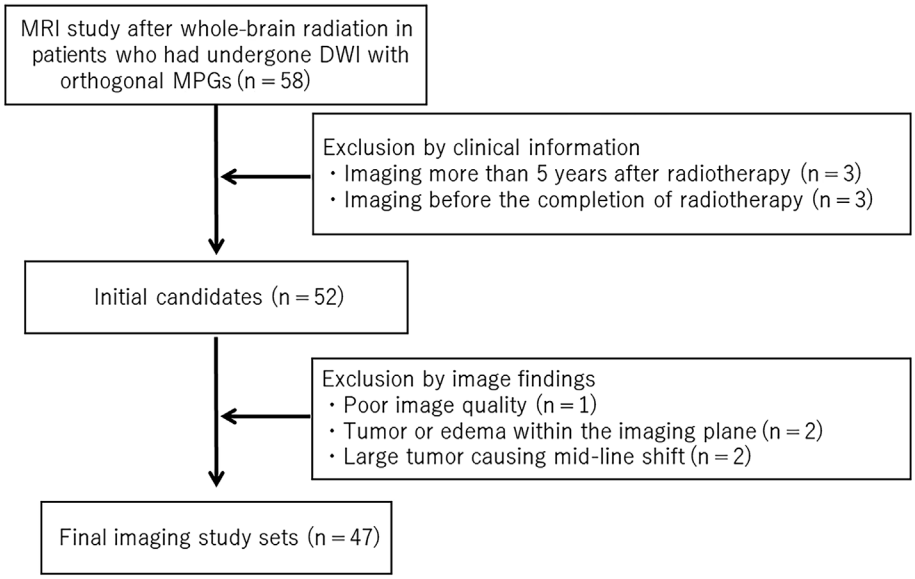

FIGURE 1 Flowchart of the patient selection procedure along with the inclusion and exclusion criteria. DWI, diffusion-weighted imaging; MPG, motion-probing gradient.

TABLE 1 The age and sex distribution of the normal control and postradiation groups.

	Normal control group		Postradiation group	
Age (years)	Male	Female	Male	Female
20–39	15	20	1	3
40–59	16	18	4	0
60–84	19	17	5	9

repetition time, 3500 ms; echo time, 95 ms; slice thickness, 5 mm; SPEEDER factor, 1.0; ETL, 9; acquisition matrix, 256 × 320; reconstruction matrix, 640 × 640; FOV, 20 cm; number of averages, one; acquisition time, 53 s; axial imaging plane on the AC-PC line.

2.2.2 | Image data analysis

Image data analysis to obtain the DWI-ALPS index was performed using the same method as reported in previously published work.[14] We retrospectively generated apparent diffusion coefficient (ADC) images with the MPGs in the *x*-, *y*-, and *z*-axes, and created composite color images from the $b = 0$ images and the ADC images in the manner with the *x*-axis = red, *y*-axis = green, and *z*-axis = blue. On the slice including the body of the lateral ventricle of the composite color image, we identified the projection fiber and association fiber areas and measured ADC values along the *x*-, *y*-, and *z*-axes. We calculated the DWI-ALPS index, which is given by the ratio of the mean of the *x*-axis ADC in the area of the projection fiber (ADCxproj) and the *x*-axis ADC in the area of association fibers (ADCxassoc) to the mean of the *y*-axis ADC in the area of the projection fiber (ADCyproj) and *z*-axis ADC in the area of association fibers (ADCzassoc), as follows:

DWI-ALPS index = mean (ADCxproj, ADCxassoc)/mean (ADCyproj, ADCzassoc).

Generation of ADC and composite images and calculation of the DWI-ALPS index were performed using ImageJ (version 1.50b, National Institutes of Health, Bethesda, MD, USA) with a homemade macro script. Region of interest (ROI) placement and measurements were independently performed by two neuroradiologists (TT and SN).

2.3 | Statistical analysis

The following statistical analysis was conducted on the DWI-ALPS index for each case obtained using the above process. Statistical analysis and graph generation were performed using R (version 4.02).

1. Evaluation of correlations between the two observers

The correlation coefficients of the measurements of the two observers were calculated for the DWI-ALPS index measured for all 152 imaging sets, including 47 imaging sets of the postradiation group and 105 imaging sets of the normal control group using Pearson's correlation analysis. The final DWI-ALPS index for the subsequent evaluation was defined as the average value of the two observers' measurements.

2. Comparison between the postradiation and normal control groups

First, comparisons were made between the postradiation and normal control groups in total using a *t*-test. Comparisons were also made for sex differences. An analysis of covariance was performed to evaluate the effect of age as a covariate for the postradiation and normal control groups. Stratified analysis was conducted in three age groups consisting of 20–39, 40–59, and 60–84 years.

3. Evaluation of the relationship between the DWI-ALPS index and radiation dose

To examine the relationship between radiation dose and DWI-ALPS index, biologically equivalent doses (BEDs) were used as indices of radiation dose.[20–22] The BED is expressed by the following equation:

$$BED = D(1 + d/[\alpha/\beta]),$$

where D is the total dose and d is the single dose. α and β represent the intrinsic radiosensitivity of irradiated cells, and the α / β ratio is a measure of the fractionation sensitivity of the cells.[23] An α / β ratio of 2 was applied in this study; $\alpha/\beta = 2$ is commonly accepted for the brain as a late-reacting tissue.[24]

The correlation between BED and the ALPS index was evaluated using Pearson's correlation analysis. The evaluation was made for the entire postradiation group and was stratified into three groups: 20–39, 40–59, and 60–84 years.

4. Evaluation of the relationship between the DWI-ALPS index and postradiation duration

Correlations between postradiation duration and the DWI-ALPS index were evaluated using Pearson's correlation analysis, and correlation coefficients were calculated. Also, for this evaluation, the postradiation group was stratified into three age groups: 20–39, 40–59, and 60–84 years.

5. Evaluation of the relationship between the DWI-ALPS index and white matter T2 hyperintensity

Correlations between the DWI-ALPS index and white matter T2 hyperintensity were assessed using the Fazekas scale, including periventricular white matter (PVWM) grade and deep white matter (DWM) grade, were evaluated using the Spearman rank correlation test. Evaluations were performed on all patients including the normal control and postradiation groups, on the normal control group only, and on the postradiation group only.

3 | RESULTS

1. Evaluation of correlations between the two observers

Figure 2 shows the correlation between two independent measurements of the DWI-ALPS index by the two observers, with two-sided 95% confidence intervals. The correlation coefficient between the measurements of the two observers was 0.862 for all measurements. The correlation coefficient limited to the normal control and postradiation groups was 0.861 and 0.836, respectively.

2. Comparison between postradiation and normal control groups

In the comparison of imaging sets including all age groups, the ALPS index was significantly lower ($p < 0.001$) in the postradiation group (mean ± SD, 1.32 ± 0.16) than in the normal control group (1.44 ± 0.17) (Figure 3A). There were no statistically significant differences in the ALPS index for males and females both in the postradiation group (male: 1.28 ± 0.14, female: 1.28 ± 0.14; $p = 0.22$) and in the normal control group (male: 1.46 ± 0.14, female: 1.42 ± 0.14; $p = 0.29$). In the trial for analysis of covariance to evaluate the effect of age as a covariate, the regression coefficient was −0.0057 for the postradiation group and −0.0026 for the normal control group. There was a significant interaction ($p = 0.037$) between the group variables (postradiation and normal control groups) and age (Figure 3B). Thus, covariance analysis could not be performed because of significant interactions between group variables and covariates. So, we performed stratified analysis for three age groups consisting of 20–39, 40–59, and 60–84 years.

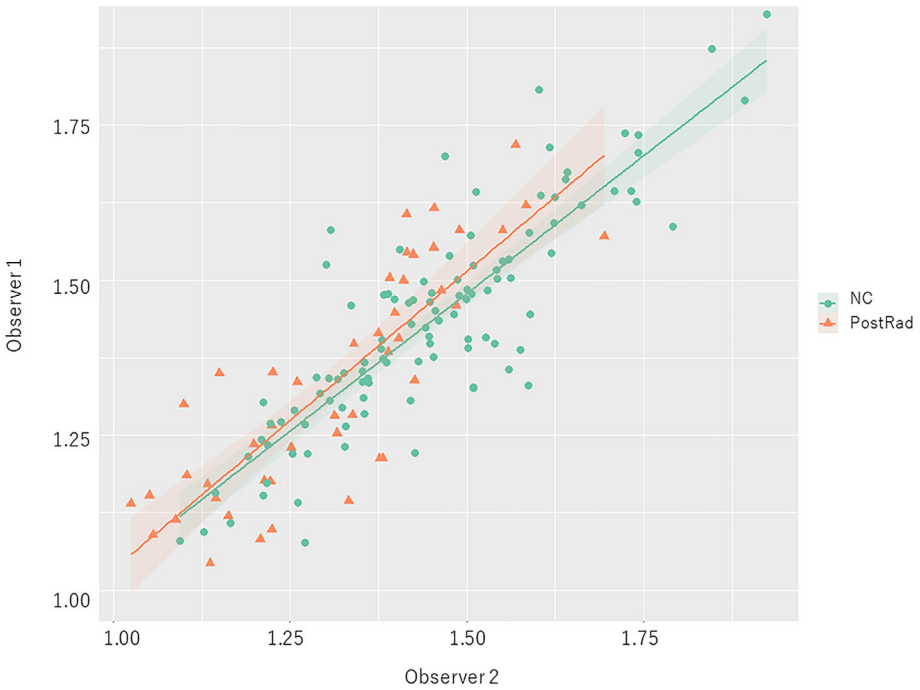

FIGURE 2 Correlation between two independent measurements by the two observers. The DWI-ALPS index measured by the two independent observers is plotted (red: postradiation group, green: normal control group). Two-sided 95% confidence intervals are shown. The correlation coefficients between the two observers were 0.862 overall, 0.861 for the normal control group, and 0.836 for the postradiation group. The data for the normal control group consisted of 105 imaging sets from 105 cases, which are part of already published data that included participants aged older than 20 years.[14] DWI-ALPS, diffusion-weighted image analysis along the perivascular space; NC, normal control group; PostRad, postradiation group.

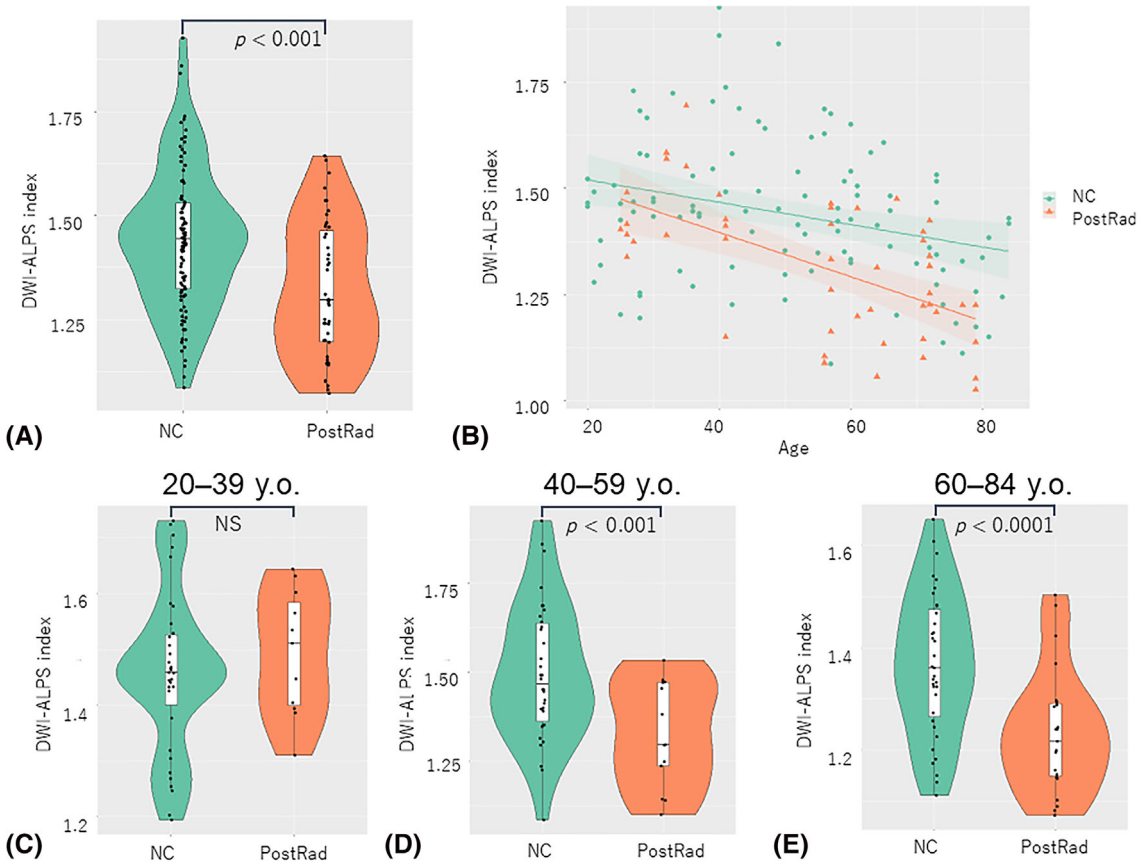

FIGURE 3 DWI-ALPS index of the postradiation group and the normal control group. (A) Comparison of DWI-ALPS index values for the whole age group. The DWI-ALPS index was significantly ($p < 0.001$) lower in the postradiation group than in the normal control group. (B) Analysis of covariance (ANCOVA) to evaluate the effect of age as a covariate. Correlation between the DWI-ALPS index and the age is plotted. There was a significant interaction ($p = 0.037$) between group variables (irradiated and normal cases) and age. (C) Stratified analysis of the 20–39 years age group. The DWI-ALPS index values of the postradiation (1.49 ± 0.11) and normal control groups (1.46 ± 0.14) showed no significant difference. (D) Stratified analysis of the 40–59 years age group. The DWI-ALPS index values of the postradiation group (1.32 ± 0.15) was significantly ($p < 0.001$) lower than that of the normal control group (1.50 ± 0.19). (E) Stratified analysis of the 60–84 years age group. The DWI-ALPS index of the postradiation group (1.23 ± 0.12) was statistically significantly ($p < 0.0001$) lower than that of the normal control group (1.37 ± 0.14). DWI-ALPS, diffusion-weighted image analysis along the perivascular space; NC, normal control group; PostRad, postradiation group.

Stratified analysis of age groups revealed that in the 20–39-year-old participants, the ALPS index of the postradiation (1.49 ± 0.11) and normal control (1.46 ± 0.14) groups showed no significant difference (Figure 3C). However, in the 40–59-year-old group, the ALPS index of the postradiation group (1.32 ± 0.15) was significantly ($p < 0.001$) lower than that of the normal control group (1.50 ± 0.19) (Figure 3D). Particularly, in participants aged 60–84 years, the ALPS index of the postradiation group (1.23 ± 0.12) was significantly ($p < 0.0001$) lower than that of the normal control group (1.37 ± 0.14) (Figure 3E).

3. Evaluation of the relationship between the DWI-ALPS index and radiation dose

In all cases of the postradiation group, the correlation with BED was calculated and showed a very weak negative correlation of $r = -0.19$ (Figure 4). The results according to age group were as follows: 20–39 years, $r = 0.22$; 40–59 years, $r = -0.25$; and 60–84 years, $r = -0.17$.

4. Evaluation of the relationship between the DWI-ALPS index and postradiation duration

In all cases in the postradiation group, the correlation with postradiation duration was calculated and showed almost no correlation ($r = 0.043$) (Figure 5). The results according to age group were as follows: 20–39 years, $r = -0.58$; 40–59 years, $r = -0.001$; and 60–84 years, $r = -0.12$.

5. Evaluation of the relationship between the DWI-ALPS index and the white matter T2 hyperintensity

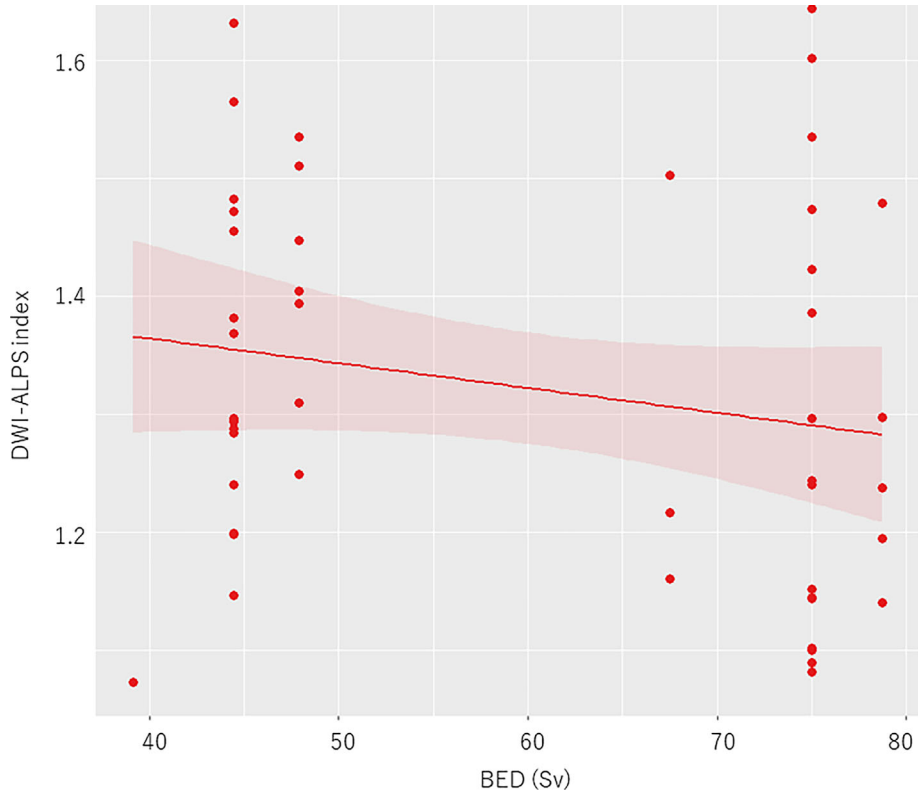

FIGURE 4 Evaluation of the relationship between the DWI-ALPS index and radiation dose. In all cases in the postradiation group, the correlation with BED showed a very weak negative correlation ($r = -0.19$). BED, biologically equivalent dose; DWI-ALPS, diffusion-weighted image analysis along the perivascular space.

In the evaluation of all patients including the normal control and postradiation groups, the results were as follows: $r = -0.46$ for PVWM and $r = -0.38$ for DWM. In the evaluation of the normal control group only, the results were as follows: $r = -0.29$ for PVWM and $r = -0.14$ for DWM. In the evaluation of the postradiation group only, the results were as follows: $r = -0.39$ for PVWM and $r = -0.40$ for DWM (Figure 6).

4 | DISCUSSION

The current study aimed to evaluate interstitial fluid dynamics in the brain using the DWI-ALPS method, which is a currently available, noninvasive method for evaluating interstitial fluid dynamics. Our findings revealed that the postradiation group exhibited a lower ALPS index than the normal control group.

In 2012, the glymphatic system hypothesis proposed that interstitial fluid and cerebrospinal fluid are involved in the excretion of waste products in brain tissue.[4] Since then, attention has been focused on the role of interstitial fluid in supplying substances to tissues and removing waste products from tissues. Although there are several arguments against the glymphatic system hypothesis, it is important to consider that interstitial and cerebrospinal fluids play an important role in brain function and homeostasis. Recently, intracranial fluids, including cerebrospinal fluid, interstitial fluid, and blood, have been comprehensively evaluated as "neurofluids".[5,25] In addition, the term "central nervous system (CNS) interstitial fluidopathy" has been proposed to describe diseases and conditions in which abnormal interstitial fluid dynamics are important in the disease process.[26,27] Alzheimer's disease is considered to be one of the CNS interstitial fluidopathy disorders. When amyloid-β is injected directly into brain tissue, the time course of amyloid efflux is delayed in AQP4 knockout mice, suggesting that the interstitial fluid dynamics, including AQP4 water channels, is involved in amyloid-β efflux.[4]

In the current study, the ALPS method was used for estimating interstitial fluid dynamics based on the ratio of diffusivities of water molecules in the perivascular space direction. When evaluating the diffusivity of water molecules in the brain parenchyma, especially in the white matter, it is difficult to evaluate the small diffusivity in the perivascular space direction because of the strong influence of diffusion in the large white matter fibers. However, if the direction is orthogonal to the large white matter fibers, the influence should be geometrically separable. Within the human brain, the medullary vessels and their perivascular space direction in the white matter outside the lateral ventricular body run in a transverse plane in a left–right direction. In the region close to the lateral ventricles, projection fibers, including pyramidal tracts, run in a vertical direction, and

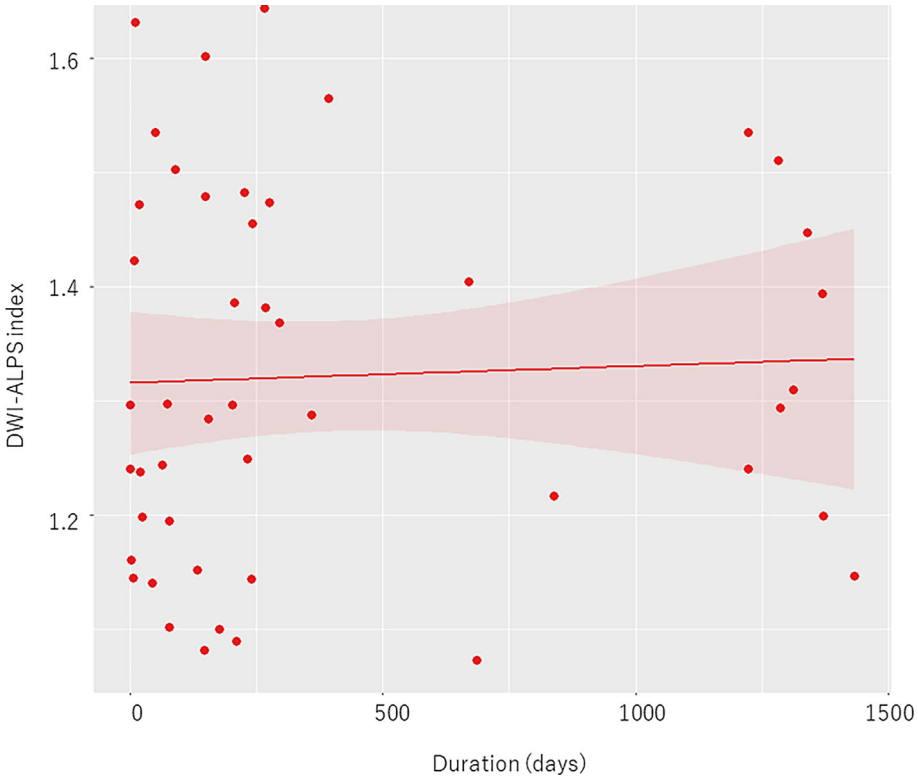

FIGURE 5 Evaluation of the relationship between the DWI-ALPS index and postradiation duration. In all cases in the postradiation group, the correlation with postradiation duration was calculated and showed almost no correlation ($r = 0.043$). DWI-ALPS, diffusion-weighted image analysis along the perivascular space.

outside of them, commissural fibers, including the superior longitudinal bundle, run in an anteroposterior direction. These run orthogonally to each other. In other words, in this region, diffusion in the perivascular space direction of the medullary arterioles can be measured geometrically separate from the diffusion effects of the large white matter fibers. The ALPS index is a mean ratio of the diffusivity in the direction of perivascular space to the internal controls. In areas where projection fibers predominated, diffusivity in the *y*-axis direction, which is orthogonal to both the projection fibers and the perivascular space, is used as an internal control.In areas where association fibers predominated, diffusivity in the *z*-axis direction, which is orthogonal to both the association fibers and the perivascular space, is used as an internal control. Thus, the ratio of water molecule diffusion in the perivascular space direction can be evaluated.[7] Most studies using the ALPS method use a *b*-value of 1000 s/mm.[18-27] In this study, a *b*-value of 1000 s/mm^2 was also used. However, it would be necessary to adopt a different *b*-value depending on the assumed object of observation. For the purpose of observing relatively fast diffusion components, a lower *b*-value is needed, and for studies that attempt to observe slow diffusion components, a higher *b*-value should be adopted.

Several factors have been proposed as causes of CNS symptoms after radiation, including triggering induction of pro-oxidative and pro-inflammatory environments, causing an imbalance in matrix metalloproteinases and extracellular matrix in the brain, and alerting physiological angiogenesis in the brain.[28] In addition, radiation therapy disrupts the blood–brain barrier (BBB), altering the functional architecture of the brain's microvasculature and increasing its permeability.[29] This mechanism is similar to the changes caused by small vessel disease. Small vessel disease is largely associated with loss of arterial elasticity, markedly reduced arterial compliance, and reduced autonomic nervous system function, which leads to diffuse rarefaction of myelin sheaths, followed by axonal disruption and severe astrocyte gliosis.[30] These are suggested to cause disturbances in the interstitial fluid dynamics.

In the current study, a linear correlation with age showed a negative correlation between the postradiation and normal control groups. A particularly strong negative correlation was observed in the postradiation group. Evaluation of the relationship with the BED in the postradiation group revealed that the ALPS index had a very weak negative correlation with the dose. There was no clear correlation between postradiation duration and the ALPS index. These results suggest that the postradiation group possessed abnormal interstitial fluid dynamics compared with the normal control group. In particular, the degree of abnormal interstitial fluid dynamics was more pronounced in older individuals than in the younger population. However, the dose and postradiation duration were observed to have a limited impact on changes in interstitial fluid dynamics.

White matter hyperintensity is an abnormal T2 signal in the white matter visualized on MRI that is associated with pathological conditions including hypertension, cerebrovascular disease, neuroinflammation, and aging. It is recognized as an important associated factor of cognitive decline and dementia.[31–33] We evaluated high signals on T2-weighted images of the white matter using the Fazekas scale, which has been reported to correspond to distinct ranges of quantitative white matter volume with relatively little overlap.[34] In the current study, the evaluation

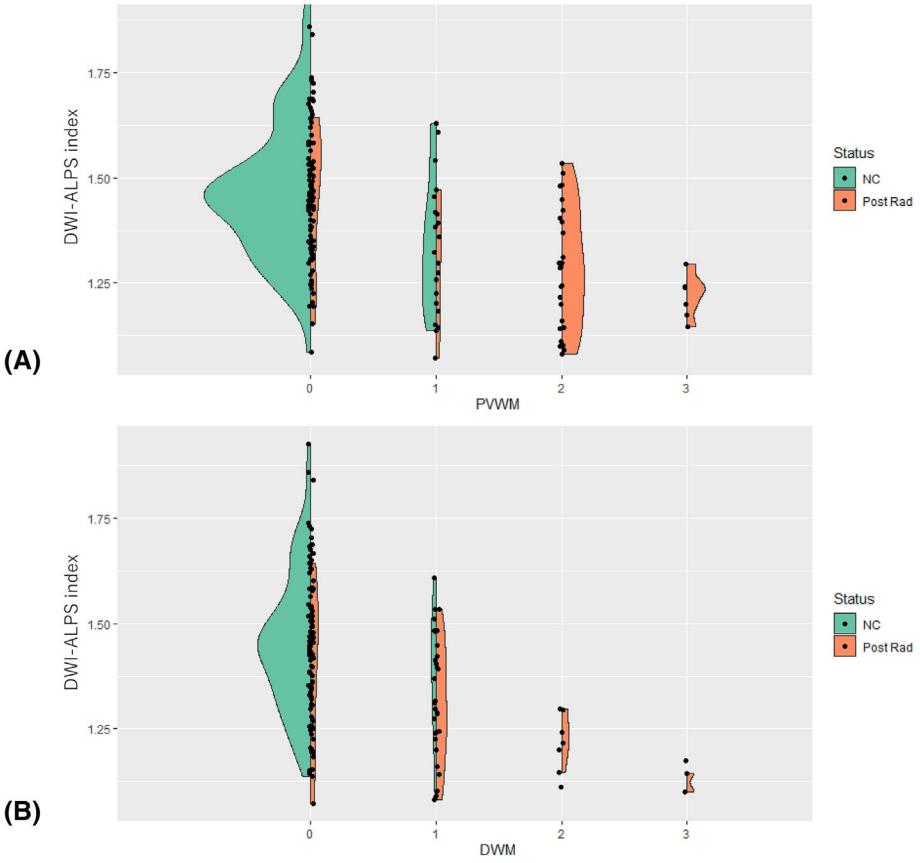

FIGURE 6 Evaluation of the relationship between the DWI-ALPS index and the white matter T2 hyperintensity. (A) Evaluation of PVWM grade. In the evaluation of all patients in the normal control and postradiation groups, significant negative correlation ($r = -0.46$) was observed. In the evaluation of the normal control group only, weak negative correlation ($r = -0.29$) was observed. In the evaluation of the postradiation group only, moderate negative correlation ($r = -0.39$) was observed. (B) Evaluation of DWM grade. In the evaluation of all patients in the normal control and postradiation groups, moderate negative correlation ($r = -0.38$) was observed. In the evaluation of the normal control group only, very weak negative correlation ($r = -0.14$) was observed. In the evaluation of the postradiation group only, significant negative correlation ($r = -0.40$) was observed. DWI-ALPS, diffusion-weighted image analysis along the perivascular space; DWM, deep white matter; NC, normal control group; PostRad, postradiation group; PVWM, periventricular white matter.

of all patients, including the normal control and postradiation groups, showed that the DWI-ALPS index had a negative correlation with the Fazekas scale in both the PVWM and DWM. These results suggest that a lower DWI-ALPS index may be correlated with the underlying pathological status of the brain white matter, which is visible as white matter hyperintensity on T2-weighted images.

In radiotherapy of the CNS, it is important to note the deterioration of brain function, especially cognitive function, which is caused by radiation at doses that are usually considered tolerable. The suggested pathogenesis of cognitive decline following radiation therapy includes cerebrovascular damage, which causes BBB disruption, neuroanatomical changes such as alterations in dendritic spine density and morphology or neuronal architecture, and impairment of neurogenesis and neuroinflammation.[35] Radiation activates astrocytes and microglia, leading to neuroinflammation and reactive gliosis.[36] Increased tumor necrosis factor α activity leads to BBB breakdown and immune cell activation.[37] Therefore, changes in the tissue environment, including interstitial fluid dynamics, may be involved in the development of cognitive symptoms after whole-brain radiation. When considering the radiation response of the brain, age is an important factor. Animal studies have revealed that, unlike young adult rats, older rats do not show a sustained decrease in the number of immature neurons after whole-brain radiation but display a greater inflammatory response. Inflammatory responses may play an important role in the development of radiation-induced cognitive dysfunction in the elderly.[38] The inflammatory response to radiation may be related to metabolic overload beyond the reserve capacity of aged rat brain tissues. In clinical practice, it is known that aging is an important risk factor for cognitive decline in patients undergoing whole-brain radiation.[39–41] When stereotactic radiation is used for brain metastases, the addition of whole-brain radiation may affect higher brain functions, such as cognitive impairment.[42,43] As shown in the results of the current study, the trend towards a lower ALPS index in older participants of the postradiation group, that is, the presence of impaired interstitial fluid dynamics, appears to be a common result of the whole-brain radiation described earlier. The current study suggests an impairment of interstitial fluid dynamics in patients presenting with alterations of the ALPS index after whole-brain radiotherapy. Our findings add to the evidence that whole-brain radiotherapy may affect interstitial fluid dynamics in the brain.

The current study has several limitations. First, we conducted a retrospective evaluation, and the number of cases was small. Moreover, because of the retrospective nature of the study, the assessment of each patient's cognitive symptoms was incomplete. In the future, a prospective study should be conducted with a larger cohort that includes evaluation of cognitive symptoms. Another limitation is the lack of evaluation of concurrent treatments such as chemotherapy. These factors may have affected the ALPS index and other results. One fundamental limitation of this study is the use of the ALPS method to assess interstitial fluid dynamics, because the ALPS method has several limitations. One is that the ALPS index measurements are affected by the imaging plane and head position.[13] In this regard, a method to retrospectively correct the angle has been proposed[44]; however, because this study used DWI data, retrospective correction could not be applied. In addition, the manual ROI setting was unstable and could have potentially affected the ALPS index measurements. A proposed solution is to standardize the images to MNI coordinates[11]; however, this method could not be applied to the DWI data in the current study. While the ALPS method uses diffusion images and thus can acquire images in a relatively short time, it should also be recognized that it is affected by physiological noise such as cardiac pulse or respiration, which may be related to variations in the data. The ALPS method has also been criticized for its lack of validation. To address this issue, good correlation has been reported in comparison with the intrathecal administration of gadolinium-based contrast agents.[10]

In conclusion, alterations in interstitial fluid dynamics were observed in patients after whole-brain radiotherapy using the ALPS method. In older populations, including the 40–59- and 60–84-year-old age groups, the ALPS index was significantly lower in the whole-brain radiation cases than in normal controls, suggesting that abnormal interstitial fluid dynamics after whole-brain radiation are associated with age. On the other hand, only a slight negative correlation between total dose and the ALPS index was observed, and no correlation between duration after radiation and the ALPS index was observed. Further systematic prospective studies are required to investigate their association with cognitive symptoms.

CONFLICT OF INTEREST STATEMENT

The Department of Innovative Biomedical Visualization (iBMV), Nagoya University Graduate School of Medicine, was financially supported by the Canon Medical Systems Corporation.

ETHICS STATEMENT

This retrospective study was performed with the approval of the Institutional Review Board of Nagoya University (2021-0228).

ORCID


Toshiaki Taoka https://orcid.org/0000-0001-9227-0240

REFERENCES

1. Garsa A, Jang JK, Baxi S, et al. Radiation therapy for brain metastases: a systematic review. *Pract Radiat Oncol*. 2021;11(5):354-365. doi:10.1016/j.prro.2021.04.002
2. Ferreri AJM. Therapy of primary CNS lymphoma: role of intensity, radiation, and novel agents. *Hematology Am Soc Hematol Educ Program*. 2017;2017(1):565-577. doi:10.1182/asheducation-2017.1.565
3. Laack NN, Brown PD. Cognitive sequelae of brain radiation in adults. *Semin Oncol*. 2004;31(5):702-713. doi:10.1053/j.seminoncol.2004.07.013
4. Iliff JJ, Wang M, Liao Y, et al. A paravascular pathway facilitates CSF flow through the brain parenchyma and the clearance of interstitial solutes, including amyloid beta. *Sci Transl Med*. 2012;4(147):147ra111. doi:10.1126/scitranslmed.3003748
5. Agarwal N, Contarino C, Toro EF. Neurofluids: a holistic approach to their physiology, interactive dynamics and clinical implications for neurological diseases. *Veins and Lymphatics*. 2019;8(3):8470. doi:10.4081/vl.2019.8470
6. Naganawa S, Taoka T. The glymphatic system: a review of the challenges in visualizing its structure and function with MR imaging. *Magn Reson Med Sci*. 2022;21(1):182-194. doi:10.2463/mrms.rev.2020-0122
7. Taoka T, Masutani Y, Kawai H, et al. Evaluation of glymphatic system activity with the diffusion MR technique: diffusion tensor image analysis along the perivascular space (DTI-ALPS) in Alzheimer's disease cases. *Jpn J Radiol*. 2017;35(4):172-178. doi:10.1007/s11604-017-0617-z
8. Yokota H, Vijayasarathi A, Cekic M, et al. Diagnostic performance of glymphatic system evaluation using diffusion tensor imaging in idiopathic normal pressure hydrocephalus and mimickers. *Curr Gerontol Geriatr Res*. 2019;2019:5675014. doi:10.1155/2019/5675014
9. Chen HL, Chen PC, Lu CH, et al. Associations among cognitive functions, plasma DNA, and diffusion tensor image along the perivascular space (DTI-ALPS) in patients with Parkinson's disease. *Oxid Med Cell Longev*. 2021;2021:4034509. doi:10.1155/2021/4034509
10. Zhang W, Zhou Y, Wang J, et al. Glymphatic clearance function in patients with cerebral small vessel disease. *Neuroimage*. 2021;238:118257. doi:10.1016/j.neuroimage.2021.118257
11. Kamagata K, Andica C, Takabayashi K, et al. Association of MRI indices of glymphatic system with amyloid deposition and cognition in mild cognitive impairment and Alzheimer disease. *Neurology*. 2022;99(24):e2648-e2660. doi:10.1212/WNL.0000000000201300
12. Kikuta J, Kamagata K, Takabayashi K, et al. An investigation of water diffusivity changes along the perivascular space in elderly subjects with hypertension. *Am J Neuroradiol*. 2022;43(1):48-55. doi:10.3174/ajnr.A7334
13. Taoka T, Ito R, Nakamichi R, et al. Reproducibility of diffusion tensor image analysis along the perivascular space (DTI-ALPS) for evaluating interstitial fluid diffusivity and glymphatic function: CHanges in Alps index on Multiple conditiON acquIsition eXperiment (CHAMONIX) study. *Jpn J Radiol*. 2022;40(2):147-158. doi:10.1007/s11604-021-01187-5
14. Taoka T, Ito R, Nakamichi R, et al. Diffusion-weighted image analysis along the perivascular space (DWI-ALPS) for evaluating interstitial fluid status: age dependence in normal subjects. *Jpn J Radiol*. 2022;40(9):894-902. doi:10.1007/s11604-022-01275-0

15. Lin LP, Su S, Hou W, et al. Glymphatic system dysfunction in pediatric acute lymphoblastic leukemia without clinically diagnosed central nervous system infiltration: a novel DTI-ALPS method. *Eur Radiol*. 2023;33(5):3726-3734. doi:10.1007/s00330-023-09473-8
16. Saito Y, Hayakawa Y, Kamagata K, et al. Glymphatic system impairment in sleep disruption: diffusion tensor image analysis along the perivascular space (DTI-ALPS). *Jpn J Radiol*. 2023. doi:10.1007/s11604-023-01463-6
17. Saito Y, Kamagata K, Andica C, et al. Glymphatic system impairment in corticobasal syndrome: diffusion tensor image analysis along the perivascular space (DTI-ALPS). *Jpn J Radiol*. 2023. doi:10.1007/s11604-023-01454-7
18. Yang DX, Sun Z, Yu MM, et al. Associations of MRI-derived glymphatic system impairment with global white matter damage and cognitive impairment in mild traumatic brain injury: a DTI-ALPS study. *J Magn Reson Imaging*. 2023. doi:10.1002/jmri.28797
19. Yamada K, Kizu O, Kubota T, et al. The pyramidal tract has a predictable course through the centrum semiovale: a diffusion-tensor based tractography study. *J Magn Reson Imaging*. 2007;26(3):519-524. doi:10.1002/jmri.21006
20. Barendsen GW. Dose fractionation, dose rate and iso-effect relationships for normal tissue responses. *Int J Radiat Oncol Biol Phys*. 1982;8(11):1981-1997. doi:10.1016/0360-3016(82)90459-x
21. Fowler JF. The linear-quadratic formula and progress in fractionated radiotherapy. *Br J Radiol*. 1989;62(740):679-694. doi:10.1259/0007-1285-62-740-679
22. Withers HR, Thames HD Jr, Peters LJ. A new isoeffect curve for change in dose per fraction. *Radiother Oncol*. 1983;1(2):187-191. doi:10.1016/s0167-8140(83)80021-8
23. van Leeuwen CM, Oei AL, Crezee J, et al. The alfa and beta of tumours: a review of parameters of the linear-quadratic model, derived from clinical radiotherapy studies. *Radiat Oncol*. 2018;13(1):96. doi:10.1186/s13014-018-1040-z
24. Santacroce A, Kamp MA, Budach W, Hanggi D. Radiobiology of radiosurgery for the central nervous system. *Biomed Res Int*. 2013;2013:362761. doi:10.1155/2013/362761
25. Taoka T, Naganawa S. Neurofluid dynamics and the glymphatic system: a neuroimaging perspective. *Korean J Radiol*. 2020;21(11):1199-1209. doi:10.3348/kjr.2020.0042
26. Taoka T, Ito R, Nakamichi R, Nakane T, Kawai H, Naganawa S. Interstitial fluidopathy of the central nervous system: an umbrella term for disorders with impaired neurofluid dynamics. *Magn Reson Med Sci*. 2022. doi:10.2463/mrms.rev.2022-0012
27. Taoka T, Naganawa S. Imaging for central nervous system (CNS) interstitial fluidopathy: disorders with impaired interstitial fluid dynamics. *Jpn J Radiol*. 2021;39(1):1-14. doi:10.1007/s11604-020-01017-0
28. Lee YW, Cho HJ, Lee WH, Sonntag WE. Whole brain radiation-induced cognitive impairment: pathophysiological mechanisms and therapeutic targets. *Biomol Ther*. 2012;20(4):357-370. doi:10.4062/biomolther.2012.20.4.357
29. Diserbo M, Agin A, Lamproglou I, et al. Blood-brain barrier permeability after gamma whole-body irradiation: an in vivo microdialysis study. *Can J Physiol Pharmacol*. 2002;80(7):670-678. doi:10.1139/y02-070
30. Moretti R, Caruso P. An iatrogenic model of brain small-vessel disease: post-radiation encephalopathy. *Int J Mol Sci*. 2020;21(18):6506. doi:10.3390/ijms21186506
31. Debette S, Markus HS. The clinical importance of white matter hyperintensities on brain magnetic resonance imaging: systematic review and meta-analysis. *BMJ*. 2010;341(jul26 1):c3666. doi:10.1136/bmj.c3666
32. Wardlaw JM, Valdes Hernandez MC, Munoz-Maniega S. What are white matter hyperintensities made of? Relevance to vascular cognitive impairment. *J Am Heart Assoc*. 2015;4(6):001140. doi:10.1161/JAHA.114.001140
33. Wang M, Norman JE, Srinivasan VJ, Rutledge JC. Metabolic, inflammatory, and microvascular determinants of white matter disease and cognitive decline. *Am J Neurodegener Dis*. 2016;5(5):171-177.
34. Andere A, Jindal G, Molino J, et al. Volumetric white matter hyperintensity ranges correspond to Fazekas scores on brain MRI. *J Stroke Cerebrovasc Dis*. 2022;31(4):106333. doi:10.1016/j.jstrokecerebrovasdis.2022.106333
35. Lehrer EJ, Jones BM, Dickstein DR, et al. The cognitive effects of radiotherapy for brain metastases. *Front Oncol*. 2022;12:893264. doi:10.3389/fonc.2022.893264
36. Kanzawa T, Iwado E, Aoki H, et al. Ionizing radiation induces apoptosis and inhibits neuronal differentiation in rat neural stem cells via the c-Jun NH2-terminal kinase (JNK) pathway. *Oncogene*. 2006;25(26):3638-3648. doi:10.1038/sj.onc.1209414
37. Wilson CM, Gaber MW, Sabek OM, Zawaski JA, Merchant TE. Radiation-induced astrogliosis and blood-brain barrier damage can be abrogated using anti-TNF treatment. *Int J Radiat Oncol Biol Phys*. 2009;74(3):934-941. doi:10.1016/j.ijrobp.2009.02.035
38. Schindler MK, Forbes ME, Robbins ME, Riddle DR. Aging-dependent changes in the radiation response of the adult rat brain. *Int J Radiat Oncol Biol Phys*. 2008;70(3):826-834. doi:10.1016/j.ijrobp.2007.10.054
39. Brandes AA, Rigon A, Monfardini S. Radiotherapy of the brain in elderly patients. *Eur J Cancer*. 2000;36(4):447-451. doi:10.1016/s0959-8049(99)00322-6
40. Swennen MH, Bromberg JE, Witkamp TD, Terhaard CH, Postma TJ, Taphoorn MJ. Delayed radiation toxicity after focal or whole brain radiotherapy for low-grade glioma. *J Neurooncol*. 2004;66(3):333-339. doi:10.1023/b:neon.0000014518.16481.7e
41. Omuro AM, Ben-Porat LS, Panageas KS, et al. Delayed neurotoxicity in primary central nervous system lymphoma. *Arch Neurol*. 2005;62(10):1595-1600. doi:10.1001/archneur.62.10.1595
42. Chang EL, Wefel JS, Hess KR, et al. Neurocognition in patients with brain metastases treated with radiosurgery or radiosurgery plus whole-brain irradiation: a randomised controlled trial. *Lancet Oncol*. 2009;10(11):1037-1044. doi:10.1016/S1470-2045(09)70263-3
43. Brown PD, Jaeckle K, Ballman KV, et al. Effect of radiosurgery alone vs radiosurgery with whole brain radiation therapy on cognitive function in patients with 1 to 3 brain metastases: a randomized clinical trial. *JAMA*. 2016;316(4):401-409. doi:10.1001/jama.2016.9839
44. Tatekawa H, Matsushita S, Ueda D, et al. Improved reproducibility of diffusion tensor image analysis along the perivascular space (DTI-ALPS) index: an analysis of reorientation technique of the OASIS-3 dataset. *Jpn J Radiol*. 2022;41(4):393-400. doi:10.1007/s11604-022-01370-2

How to cite this article: Taoka T, Ito R, Nakamichi R, et al. Evaluation of alterations in interstitial fluid dynamics in cases of whole-brain radiation using the diffusion-weighted image analysis along the perivascular space method. *NMR in Biomedicine*. 2023;e5030. doi:10.1002/nbm.5030